V_{OC} Degradation in TF-VLS Grown InP Solar Cells

Yubo Sun[1], Xingshu Sun[1], Steve Johnston[2], Carolin M. Sutter-Fella[3,4], Mark Hettick[3,4], Ali Javey[3,4] and Peter Bermel[1]

[1] Electrical and Computer Engineering, Purdue University, West Lafayette, IN, 47907, U.S.A.

[2] National Renewable Energy Laboratory, Golden, CO, 80401, U.S.A.

[3] Electrical Engineering and Computer Sciences, University of California, Berkeley, CA, 94720, U.S.A.

[4] Material Sciences Division, Lawrence Berkeley National Laboratory, Berkeley, CA, 94720, U.S.A.

***Abstract* — Here we consider two hypotheses to explain the open-circuit voltage (*Voc*) degradation observed in thin-film vapor-liquid-solid (*TF-VLS*) grown p-type *InP* photovoltaic cells: bandgap narrowing and local shunting. First, a bandgap (E_g) narrowing effect is hypothesized, based on the surface inhomogeneity of *VLS* InP captured by the photoluminescence (*PL*) image. The PL data was used to estimate a spatially-resolved active V_{OC} across surface of the InP sample. Combining this data with the effective *Jsc* allowed an assessment of the *I-V* characteristics of individual unit cells. Next, an `H-SPICE` diode compact model was utilized to reproduce the *I-V* characteristics of the whole sample. We find a good fit to the *I-V* performance of *TF-VLS* grown InP solar cell. Second, a local shunting effect was also considered as an alternative explanation of the V_{OC} degradation effect. Again, PL image data was used, and small local shunt resistance was added in arbitrary elementary unit cells to represent certain dark spots seen in the *PL* image and dictate the V_{OC} degradation occurred in the sample.**

***Index Term* — III-V semiconductor materials, thin film vapor liquid solid growth, numerical modeling, photoluminescence.**

I. Introduction

III-V semiconductor materials have played increasingly important roles in Concentrator Photovoltaics (*CPV*) and Space Photovoltaics. Despite the fact that state-of-the-art record solar cells are made of *III-V* compound (e.g. *GaAs* for single junction and *InGaP/GaAs* for tandem junction) [1], *c-Si* remains the dominant *PV* material candidate in the solar cell market. High capital expense and scaling challenges have prevented *III-V* materials from becoming the predominant choice in the *PV* market. Thus, it is crucial to explore more cost-effective growth methods for *III-V* materials. The Vapor-Liquid-Solid (*VLS*) was brought to attention and has become a dominant option for nanostructure growth due to its simplicity, flexibility, and controllability[2]. The recently developed Thin-Film Vapor-Liquid-Solid (TF-*VLS*) growth platform presents a way of growing high quality material at significantly reduced module cost and was successfully demonstrated for InP [3]–[6]. InP has a E_g of *1.34 eV*, which is near-optimal for a single junction solar cell [7]. However, it was identified from the *I-V* characteristics that *VLS*-grown *InP* solar cells show a lower V_{OC} than champion InP cells grown by traditional metal organic chemical vapor deposition technique on epitaxial substrates [8]. In this paper, we consider the V_{OC} degradation from two different perspectives: (1) E_g narrowing and (2) local shunting.

During *TF-VLS* growth, an In film is heated in PH_3 gas and transformed to InP by diffusion of P into the liquid In followed by nucleation of InP and rapid dendritic growth of thin film InP exhibiting grains (> 100 μm) much larger than the film thickness (~3 μm) [3,4]. High optoelectronic quality *TF-VLS* InP has been demonstrated [4]. n-InP layers are doped p-type with Zn by an ex-situ doping process before the electron selective TiO_2 contact is deposited, followed by ITO as the transparent front electrode and individual cell patterning by lithography [5].

II. Methodology

To fully understand and quantify the V_{OC} degradation seen in *TF-VLS* grown *InP* solar cell, we document two hypotheses from different aspects based on the characterization outcome.

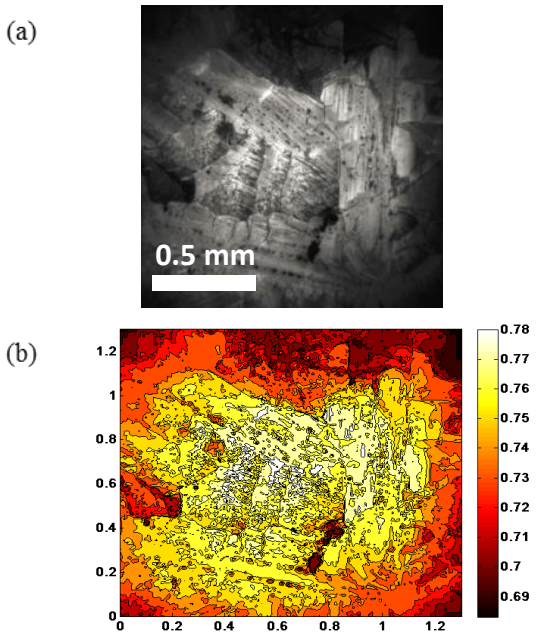

Fig. 1. (a) Photoluminescence image of *TF-VLS* grown InP solar cell (area: 1.3mm × 1.3mm) [9]. (b) Color map of the V_{OC} at each unit cell. Units in both lateral directions are in mm.

A. Bandgap Narrowing

The photoluminescence (*PL*) image of TF-VLS InP exhibits some lateral variation in PL intensity over an area of 1.3 mm ×

1.3 mm as visualized in Fig. 1a. Grain boundaries and dendritic growth pattern can be clearly seen in the millimeter scale image. In order to correlate the observed *PL* inhomogeneity and cell performance, a lateral *2D* spatially-resolved V_{OC} distribution graph was generated, based on the *PL* image. It is assumed that the luminance (a.u.) is proportional to $exp(qVoc/kT)$, with the V_{OC} obtained from single-crystal hetero-junction InP solar cell used as an upper limit (0.78 V) [10], and VLS-grown cell voltages as a lower limit (0.69 V). The V_{OC} distribution color map is generated as shown in Fig 1b. Since the sample is divided into $m \times n$ elementary unit cells, an *H-Spice* based compact model of *InP* network is constructed to combine *I-V* characteristics of elementary unit cells to reproduce the *I-V* characteristics of the *TF-VLS* grown sample.

To implement the compact model, all of the elementary unit cells are divided into two types: (1) good unit cells that have identical *I-V* performance with hetero-junction wafer based *InP* cell, and (2) bad unit cells that have degraded *I-V* performance, due to the E_g narrowing effect.

The PL image suggests that some regions may have an effective E_g smaller than the expected E_g of single crystal *InP* at the surface of our *VLS*-grown *InP* sample. There are at least several possible explanations: (1) deviation from perfect stoichiometry; (2) laterally inhomogeneous doping distributions or electron affinities; or (3) deep-level defects approximately *0.3 eV* above the valence band maximum (*VBM*). *PL* spectra of the Zn-doped *TF-VLS* grown *InP* sample taken at *T=8 K* [5] are used to quantify the effective E_g of those degraded cells. Besides the dominant band-to-band (*BB*) and band-to-acceptor (*BA*) photoluminescence, an extra peak (*BA-LO*) was also identified, which is strongly correlated with E_g narrowing. The effective E_g therefore can be extracted from our *PL* spectra. We expect that the temperature-dependent E_g will follow the Varshni relation for a semiconductor, which is given by [11]:

$$E_g(T) = E_g(0) - \propto \cdot T^2/(T+\beta),$$

where α and β are fitting parameters varied with different semiconductor materials. For *InP*, $\propto = 3.63 \times 10^{-4} eV/K$ and $\beta = 162\ K$. Because the *BA-LO* energy is *1.27 eV* as indicated in [5], the phosphorous content may be reduced roughly 5% from a 1:1 ratio in this sample. To set up the *H-Spice* compact model simulation framework for the *InP* network, threshold voltage of *0.75V* is used to split elementary unit cells in two categories. Those unit cells with local V_{OC} greater than *0.75V* are labeled as "good cells" whereas remainder unit cells are treated as "degraded cells". *I-V* characteristics of wafer-based hetero *InP* cell is modeled through *TCAD Sentaurus* as depicted in Fig 2 and implemented as local *I-V* data for "good cells". The *I-V* characteristics of degraded cells are generated by reducing the E_g from *1.34 eV* to *1.27eV* and shifting the absorption spectra accordingly while maintaining the same recombination parameter values. Two sets of *I-V* data are combined in the *H-Spice* compact model to reproduce the overall *I-V* characteristics of a *TF-VLS* grown *InP* solar cell. The energy band diagram at V_{OC} condition is also plotted in Fig 2, showing that using TiO_2 as the electron selective buffer layer in the structure creates a large valence band offset to block minority holes from reaching the electron contact, mitigating large SRH recombination in the space charge region of the *ITO* layer. The *H-Spice* diode compact model of *InP* network presumes that $m \times n$ elementary unit cells are connected in parallel to each other; sheet resistors (10Ω/□) are placed at the interconnects between any two adjacent cells. Each elementary unit cell consists of a light-generated current source and a diode. The total current *I* in the unit cell is given by:

$$I = I_{sc} - I_o \cdot \exp\left(\frac{qV}{nkT}\right),$$

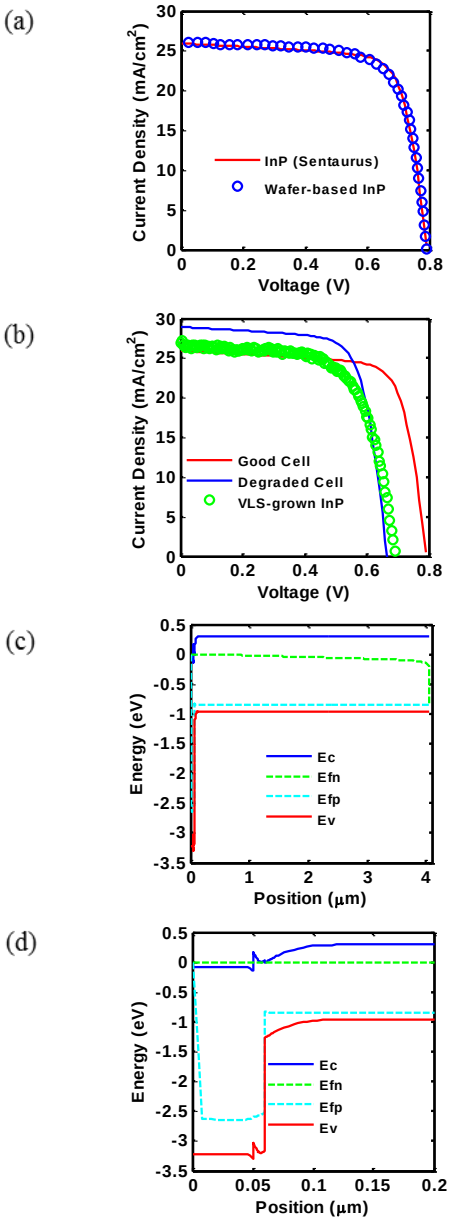

Fig. 2. (a) *TCAD Sentaurus* simulated *I-V* characteristics of wafer-based *InP* solar cell. (b) *I-V* characteristics of wafer-based *InP* implemented as local *I-V* data for non-degraded unit cells and I-V characteristics incorporating E_g narrowing effects applied as local *I-V* data for degraded unit cells. (c) and (d) are overall and zoomed-in

energy band diagrams of wafer-based *InP* solar cell plotted under V_{OC} condition with *AM1.5G* illumination.

where I_{SC} is the light generated current with no applied voltage, I_O is the reverse saturation current; n is the ideality factor. Fig 3(a) illustrates the *InP* network unit cell.

B. Local Shunting

Besides the E_g narrowing effect discussed above, elementary unit cell performance might also be degraded by low shunt resistance [12] connected in parallel with light generated current source and diode as depicted in Fig 3(a). Temperature-dependent dark *I-V* measurements of *TF-VLS* grown sample clearly exhibit shunting-dominated behavior under reverse and low forward bias condition. Note that due to some electrostatic charging and discharging effect, the dark *I-V* minima do not occur at the zero bias condition.

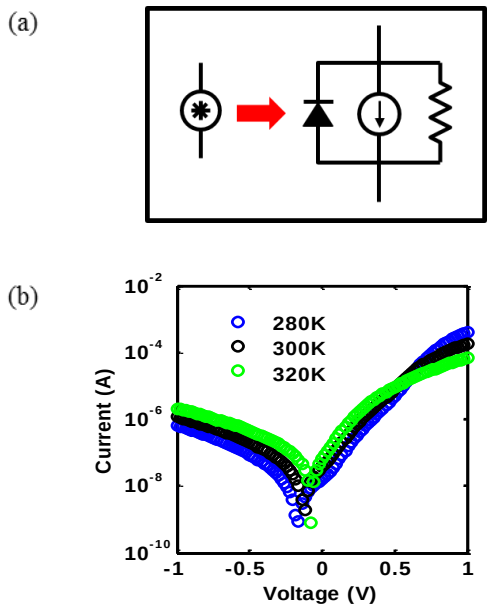

Fig. 3. (a) Internal circuit structure of elementary unit cell includes shunt resistance connected in parallel. (b) Dark *I-V* characteristics of *TF-VLS* grown *InP* measured at *280K, 300K* and *320K*.

The new diode equation, with shunt resistance included, is as follows:

$$I = I_{sc} - I_o \cdot \exp\left(\frac{qV}{nkT}\right) - \frac{V}{R_{sh}}.$$

Putting the shunt resistance in the ideal diode model would result in degradation of I-V performance, especially in the fill factor (*FF*) and V_{OC}. The degradation would not be observable unless the shunt resistance were less than *1 kΩ-cm²*. In order to model local shunt effects quantitatively, it was assumed that shunt resistance is added to unit cells that are categorized as "degraded cells". The *H-Spice* compact model of *InP* network is also constructed to produce the overall *I-V* performance of the *TF-VLS* grown sample.

III. Results and Discussion

Incorporating E_g narrowing effect in the simulation with reasonable external shunt resistance added, the resulted *I-V* has shown good agreement in V_{OC}, J_{SC} and *FF* with good curve fit to measured *I-V* characteristics of *VLS*-grown sample. The power consumptions of total unit cells are plotted under V_{OC} condition. Since unit cells are distinguished as good and degraded cells based on threshold voltage we set, while good cells are generating powers under V_{OC} condition, degraded cells start to consume power which can be clearly seen in Fig 4(b). The power consumption of degraded cells offsets the power generation of good cells at open circuit. The plots due to local shunting have shown that adding a shunt resistance in the elementary unit cell could be more harmful to current collections at small voltage bias than to the V_{OC}. And it turns out that E_g narrowing achieve much better fitting. The *FF* discrepancy in the E_g narrowing hypothesis might be as a result of the absence of shunting resistance. Therefore, adding shunt resistance to some local dark unit cells while assuming E_g narrowing for all degraded cells could optimize the *I-V* fitting.

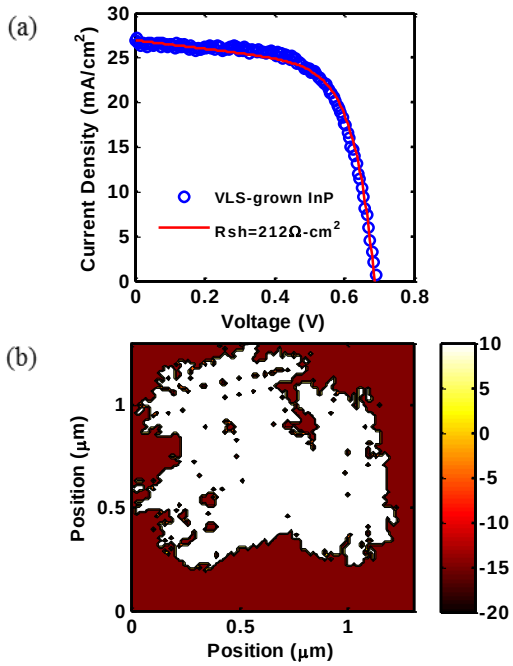

Fig. 4. (a) *I-V* characteristics of the *InP* network due to E_g narrowing shows reasonable fit to measured *I-V* of the *VLS*-grown sample. (b) Power consumption and generation of good and degraded cells in the sample at V_{OC} condition under E_g-narrowing.

Local shunting in *TF-VLS* p-InP might arise from dopant inhomogeneities and dopant clustering of non-activated Zn atoms. A dopant activation of about 10% was extracted from comparative SIMS and C-V measurements [5].

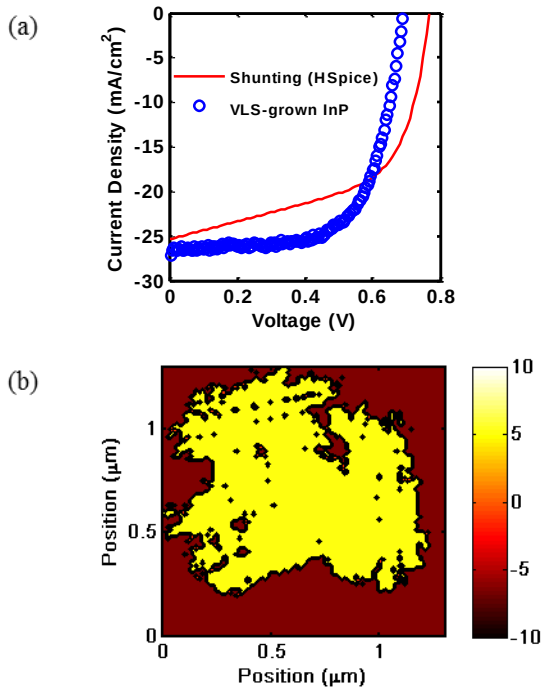

Fig. 5. (a) *I-V* characteristics of the *InP* network with shunt resistance of *50 Ω-cm²* compared to measured *I-V* characteristics of the *VLS*-grown sample. (b) Power consumption and generation of good and degraded cells in the sample at V_{OC} under local shunting.

IV. Conclusions and Future Work

In this paper, we considered two hypotheses to explain the V_{OC} degradation of *TF-VLS* grown *InP* solar cells. First, the E_g narrowing effect assumes slight deviations from 1:1 In:P stoichiometry may exist in the *InP* sample. Extracting information from various characterization results (e.g. *PL* image and *PL* spectra) and establishing *H-Spice* diode compact model based *InP* network can then be used to predict the *I-V* performance of the sample. This result achieves a good match to the measured *I-V* of *VLS* sample. Second, local shunting effect was also considered by adding shunt resistance to the individual degraded cells. It is predicted that combining two hypotheses together, optimized fitting *I-V* curves could be produced to establish a comprehensive physics based theory to explain the V_{OC} degradation in the *TF-VLS* grown *InP* solar cell. Future work should consider modeling of the random fractal network to mimic lateral dendritic polycrystalline growth pattern observed in *TF-VLS* growth process and explain the small uncertainty of measured V_{OC}. Furthermore, from the experimental perspective, an in-situ doping process is currently explored to control the doping profile better and increase the dopant activation which possibly helps eliminate local shunting in *TF-VLS* p-InP. Further improvement could be made by fabricating *VLS*-grown single crystal n-InP deposited on Moly substrate to mitigate surface inhomogeneity.

References

[1] M. A. Green, K. Emery, Y. Hishikawa, W. Warta, and E. D. Dunlop, "Solar cell efficiency tables (version 46)," *Prog Photovoltaics Res Appl*, vol. 23, no. version 46, pp. 805–812, 2015.

[2] L. Chen, W. Lu, and C. M. Lieber, "Semiconductor Nanowire Growth and Integration," in *Semiconductor Nanowires*, 2014, pp. 1–53.

[3] R. Kapadia, Z. Yu, M. Hettick, J. Xu, M. S. Zheng, C. Y. Chen, A. D. Balan, D. C. Chrzan, and A. Javey, "Deterministic nucleation of InP on metal foils with the thin-film vapor-liquid-solid growth mode," *Chem Mater*, vol. 26, no. 3, pp. 1340–1344, 2014.

[4] R. Kapadia, Z. Yu, H.-H. H. Wang, M. S. Zheng, C. Battaglia, M. Hettick, D. Kiriya, K. Takei, P. Lobaccaro, J. W. Beeman, J. W. Ager, R. Maboudian, D. C. Chrzan, and A. Javey, "A direct thin-film path towards low-cost large-area III-V photovoltaics," *Sci Rep*, vol. 3, pp. 1–7, 2013.

[5] M. Zheng, H.-P. Wang, C. M. Sutter-Fella, C. Battaglia, S. Aloni, X. Wang, J. Moore, J. W. Beeman, M. Hettick, M. Amani, W.-T. Hsu, J. W. Ager, P. Bermel, M. Lundstrom, J.-H. He, and A. Javey, "Thin-Film Solar Cells with InP Absorber Layers Directly Grown on Nonepitaxial Metal Substrates," *Adv Energy Mater*, vol. 5, p. 22, 2015.

[6] M. Zheng, K. Horowitz, M. Woodhouse, C. Battaglia, R. Kapadia, and A. Javey, "III-Vs at scale : a PV manufacturing cost analysis of the thin fi lm vapor – liquid – solid growth mode," *Prog Photovoltaics Res Appl*, vol. 24(6), no. January, pp. 871–878, 2016.

[7] L. C. Hirst and N. J. Ekins-Daukes, "Fundamental Losses in Solar Cells," *Prog Photovoltaics Res Appl*, vol. 19, pp. 286–293, 2011.

[8] C. J. Keavney, V. E. Haven, and M. Vernon, "Emitter Structures in MOCVD InP Solar Cells," *Photovoltaics Spec Conf*, pp. 141–144, 1990.

[9] S. Johnston, A. A. Motz, J. Moore, M. Zheng, A. Javey, and P. Bermel, "Photoluminescence Imaging Characterization of Thin-Film InP," in *Photovoltaics Specialist Conference 42nd*, 2015, pp. 1–6.

[10] X. Yin, C. Barraglia, Y. Lin, K. Chen, M. Hettick, M. Zheng, C. Chen, D. Kiriya, and A. Javey, "19.2% Efficient InP Heterojunction Solar Cell with Electron-Selective TiO2 Contact," *ACS Photonics*, vol. 1, no. 12, pp. 1245–1250, 2014.

[11] Y. P. Varshni, "Temperature dependence of the energy gap in semiconductors," *Physica*, vol. 34, no. 1, pp. 149–154, 1967.

[12] M. Kasemann, D. Grote, B. Walter, W. Kwapil, T. Trupke, Y. Augarten, R. A. Bardos, E. Pink, M. D. Abbott, and W. Warta, "Luminescence Imaging for Detection of Shunts on Silicon Solar Cells," *Prog Photovoltaics Res Appl*, vol. 16, pp. 297–305, 2008.